Canadian Mineralogist
Vol. 17, pp. 549-560 (1979)

HYPOTHETICAL LIQUIDUS RELATIONSHIPS IN THE SUBSYSTEM Al_2O_3–FeO–MgO PROJECTED FROM QUARTZ, ALKALI FELDSPAR AND PLAGIOCLASE FOR $a(H_2O) \leq 1$

RICHARD N. ABBOTT, JR. AND D. BARRIE CLARKE
Department of Geology, Dalhousie University, Halifax, Nova Scotia B3H 3J5

ABSTRACT

Hypothetical liquidus relationships are derived for the AFM projection (A = Al_2O_3–K_2O–Na_2O-CaO, F = FeO, M = MgO). All silicate liquids are considered to be saturated with respect to quartz, an alkali feldspar, an oligoclase–andesine and one or more of the AFM minerals, biotite, garnet, cordierite or Al_2SiO_5 (andalusite or sillimanite). The liquidus topology varies in response to changes in the subsolidus chemographic relationships. With a small number of limiting assumptions, the liquidus topologies can be specified for different regions of P–T space with $a(H_2O) \leq 1$. The derived AFM liquidus topologies provide a direct chemographic link between metamorphosed pelitic sediments and derived peraluminous magmas. The mineral assemblages and textures of certain peraluminous granites may be used to define the AFM liquidus topologies. By comparison with the hypothetical topologies, limitations can be placed on P, T and $a(H_2O)$ during crystallization. The South Mountain batholith in Nova Scotia serves as a practical example.

SOMMAIRE

On déduit des relations hypothétiques sur le liquidus pour la projection AFM (A = Al_2O_3–K_2O–NaO_2-CaO, F = FeO, M = MgO). On suppose les liquides silicatés saturés en quartz, feldspath alcalin, oligoclase ou andesine et au moins un des minéraux AFM: biotite, grenat, cordiérite et andalousite (ou sillimanite). La topologie du liquidus varie avec les relations chémographiques subsolidus. Grâce à un nombre restreint d'hypothèses, on peut déduire la topologie du liquidus pour différentes régions de l'espace P–T, dans le cas de $a(H_2O) \leq 1$. Ces topologies fournissent un lien chémographique direct entre métasédiments pélitiques et magmas hyperalumineux dérivés. Dans certains granites hyperalumineux, l'assemblage des minéraux et la texture définissent la topologie du liquidus dans le sous-système AFM. En employant les cas hypothétiques comme termes de comparaison, on parvient à fixer des limites aux valeurs que P, T et $a(H_2O)$ peuvent prendre au cours de la cristallisation. Le batholite de South Mountain (Nouvelle-Ecosse) en fournit l'exemple.

(Traduit par la Rédaction)

INTRODUCTION

The AFM projection (Thompson 1957) has been used to great advantage in showing the chemographic relationships between coexisting minerals produced in pelitic sediments during metamorphism. This paper attempts to establish the nature of the liquidus surface in the AFM system (A = Al_2O_3–K_2O–Na_2O–CaO, F = FeO, M = MgO) projected from quartz, alkali feldspar, oligoclase–andesine and H_2O. The model presented in this paper will, we hope, serve as a useful framework for discussion, subject to improvement and modification as new evidence becomes available.

It is generally believed that many batholiths crystallized from magmas produced during extreme conditions of prograde metamorphism. The initial silicate liquid is rich in normative SiO_2, $KAlSi_3O_8$ and $NaAlSi_3O_8$; these components usually make up more than 90 wt. % of the liquid. In this paper the remaining 10 wt. % is assumed to be made up of $CaAl_2Si_2O_8$, FeO, MgO, Al_2O_3 and H_2O. Other constituents such as Fe_2O_3, MnO and TiO_2 are not considered in this discussion. It is assumed throughout that the silicate liquid is saturated with respect to quartz, alkali feldspar, oligoclase (or andesine) and one or more of the AFM minerals (Al_2SiO_5, biotite, garnet or cordierite).

When two feldspars (an alkali feldspar and an oligoclase–andesine), quartz and a vapor phase (H_2O) are present, the initial silicate liquid has a temperature and composition (in terms of SiO_2, $KAlSi_3O_8$ and $NaAlSi_3O_8$) close to the liquids on the classical P–T locus of granite minima determined by Tuttle & Bowen (1958). The effect of other components such as FeO, MgO and Al_2O_3 is to lower the temperature of the minimum relative to that in the simple system SiO_2–$KAlSi_3O_8$–$NaAlSi_3O_8$–H_2O (Appendix). Thus the maximum temperature on the quartz–alkali feldspar–plagioclase–H_2O-saturated AFM liquidus is likely to be lower than the liquidus minimum in the system SiO_2–$KAlSi_3O_8$–

$NaAlSi_3O_8$–H_2O. The minimum temperature on the AFM liquidus will be at an even lower temperature but most likely not more than approximately 20°C (Appendix) below the liquidus minimum in the system SiO_2–$KAlSi_3O_8$–$NaAlSi_3O_8$–H_2O.

Only four AFM minerals are considered here: garnet, biotite, cordierite and Al_2SiO_5. The different polymorphs of Al_2SiO_5 are not specified. The experimental data that form the basis of this paper (Lee & Holdaway 1978) involved sillimanite. However, because of the very small difference in the free energies of sillimanite and andalusite, Al_2SiO_5 may be considered to be either phase without any drastic changes in the relationships discussed in this paper.

The discussion is restricted to temperatures outside the stability field of muscovite; thus, muscovite-bearing assemblages are not considered. The stability limit for muscovite used in this paper (Figs. 2-4) is from Thompson & Algor (1977).

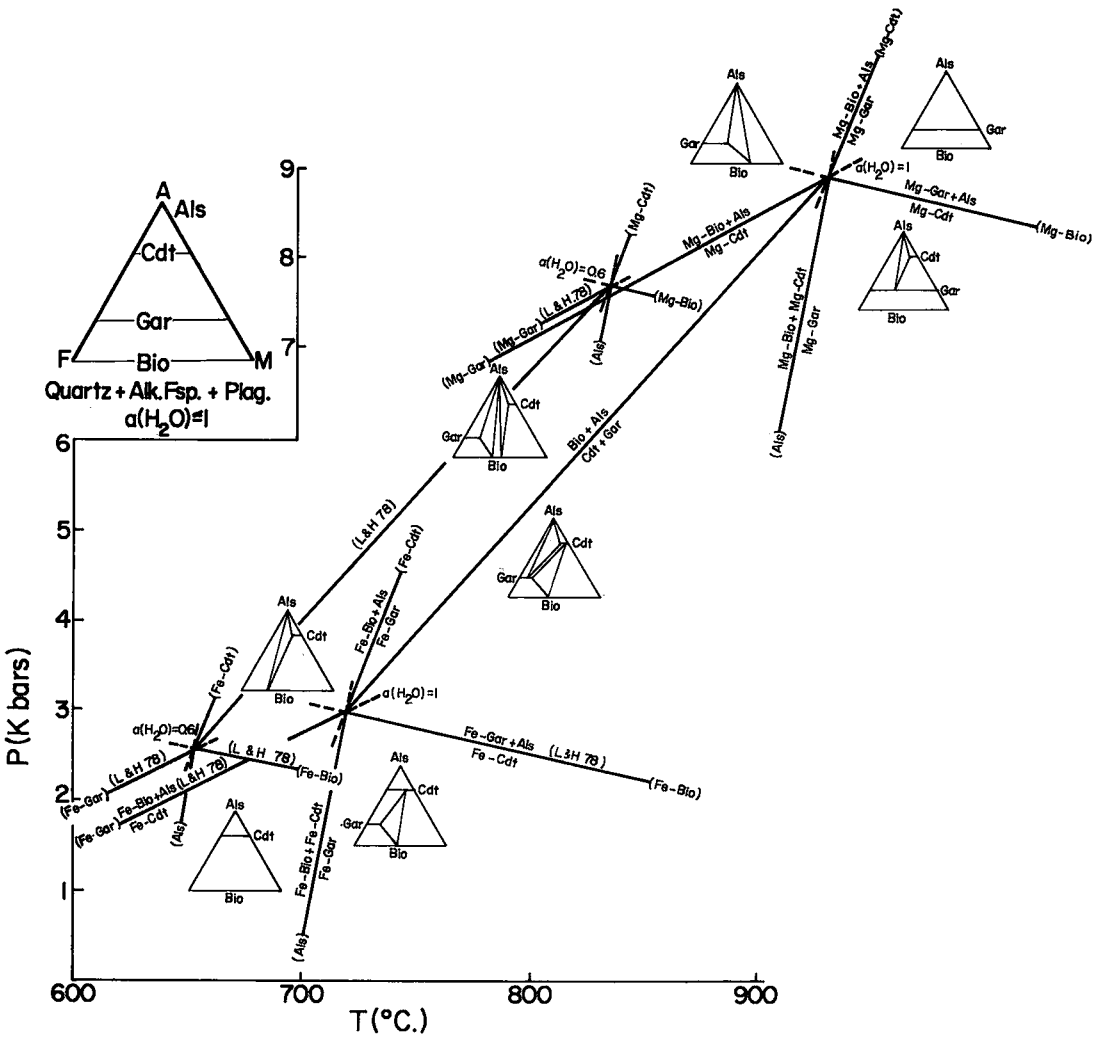

FIG. 1. Liquid-absent reactions in the system $A(Al_2O_3 - K_2O - Na_2O - CaO)$–$F(FeO)$–$(MgO)$ projected through H_2O, quartz, alkali feldspar and plagioclase for two activities of H_2O, $a(H_2O) = 1.0$ and 0.6. Reactions taken from Lee & Holdaway (1978) are marked (L & H 78). The rest of the reactions are necessitated by Schreinemakers' rules. Note that all of the reactions are shifted to lower temperatures with decreasing $a(H_2O)$. Mineral abbreviations used here and throughout the text: Als = Al_2SiO_5 (sillimanite or andalusite), Gar = garnet, Bio = biotite, Cdt = cordierite, Mus = muscovite, Liq = silicate liquid.

All reactions are written in terms of the AFM minerals only. It should be understood that quartz, alkali feldspar, oligoclase–andesine and H_2O or any combination of two or more of these species are involved in order to balance the reactions. Where a silicate liquid is involved, quartz, alkali feldspar, oligoclase–andesine and H_2O may be thought of as participating according to the following generalized reaction: quartz + alkali feldspar + plagioclase → liquid, with $a(H_2O) \leq 1$. This reaction represents an oversimplification of the possible liquidus reactions that may occur in the system SiO_2–$KAlSi_3O_8$–$NaAlSi_3O_8$–$CaAl_2Si_2O_8$–H_2O depending on P(total) and $a(H_2O)$ (Abbott 1978), but will suffice for the purposes of this paper.

Liquid-Absent Equilibria

Before discussing the liquidus relationships in the AFM projection, it is essential to know the subsolidus chemographic relationships. This section defines the subsolidus relationships as a function of P, T and $a(H_2O)$.

The Fe– and Mg–end-member subsolidus reactions involving cordierite, biotite, garnet and Al_2SiO_5 are shown in Figure 1 for two activities of H_2O, $a(H_2O) \sim P(H_2O)/P(total) = 1.0$ and 0.6. Each univariant line is labeled according to the phase not involved in the reaction. The reactions (Fe–Gar), (Fe–Bio), (Mg–Gar) and (Mg–Bio) for $a(H_2O) = 1$ and $a(H_2O) \sim 0.6$ are from Lee & Holdaway (1978). The univariant lines (Fe–Bio) and (Fe–Gar) meet at an invariant point, here labeled according to the activity of H_2O. There is an analogous invariant point for each $a(H_2O)$ in the Mg–end-member system. For a given $a(H_2O)$ the two invariant points, one each for the Fe– and Mg–end-member systems, are connected by a univariant line in the combined Fe–Mg system marking the reaction (AFM phases only):

$$\text{Bio} + Al_2SiO_5 = \text{Cdt} + \text{Gar} \qquad (1)$$

The remaining univariant lines for Fe– and Mg–end-member reactions were not included in the study by Lee & Holdaway (1978). These additional reactions, (Fe–Als), (Fe–Cdt), (Mg–Als) and (Mg–Cdt), were deduced and located relative to the other reactions according to Schreinemakers' rules. The actual slopes (dP/dT) of the additional reactions are not known, but are assumed to be positive insofar as most dehydration reactions have positive slopes ($dP/dT > 0$) within the range of pressures under consideration.

All the equilibria are shifted to lower temperatures as $a(H_2O)$ is decreased. The Fe–end-member and Mg–end-member invariant points are shown for $a(H_2O) = 1.0$ and ~ 0.6 (Lee & Holdaway 1978).

For a given $a(H_2O)$, the various equilibria in the Fe–end-member system, Mg–end-member system and Fe–Mg reaction (1) divide the P–T space into regions of topologically distinct chemographic relationships in the AFM projection. The different AFM topologies for $a(H_2O) = 1.0$ are shown in Figure 1.

Liquidus Relationships

In any ternary liquidus diagram the correct arrangement of Alkemade triangles can be deduced directly from the liquidus topology (Ehlers 1972). The minerals forming the apices of each Alkemade triangle constitute the stable subsolidus assemblage for bulk compositions within the triangle. It does not follow directly that for a given arrangement of Alkemade triangles there is a unique liquidus topology. However, it is true that for each Alkemade line connecting two mineral phases, there must be a two-phase liquidus boundary separating the primary liquidus fields for the same two phases. The two-phase liquidus boundary may be odd (peritectic) or even (cotectic) or in part odd and in part even, using the terminology of Ricci (1951). It is also true that for each Alkemade triangle relating three phases, there must be either a ternary eutectic or a ternary peritectic relating the same three mineral phases and the liquid. It follows that every change in the arrangement of the Alkemade lines, and hence every change in the subsolidus relationships, must be accompanied by a corresponding change in the liquidus topology. In the AFM projection, the tie-lines connecting stable pairs of phases in the subsolidus region behave like Alkemade lines and may be treated as such. Similarly, three-phase regions in the AFM projection correspond to Alkemade triangles.

Figure 2 shows the presumed stable equilibria where $a(H_2O) = 1$. As described earlier, the liquidus minimum in the AFM projection lies at a lower temperature than the minimum in the simple system SiO_2–$KAlSi_3O_8$–$NaAlSi_3O_8$–H_2O. Two of the Fe–end-member subsolidus reactions meet the locus of minima at two points, *f* and *c*, dividing the locus of minima into three segments. Along each segment the liquidus minimum is related to the appearance of a liquid

field in a different subsolidus AFM topology. Schematic liquidus diagrams are shown for each of the three pressure ranges, $P > c$, $f < P < c$ and $P < f$. The direction of falling temperature on the various two-phase liquidus boundaries is indicated by arrows. The placement of the two-phase liquidus boundaries and directions of falling temperature were predicted on the basis of the following assumptions: (1) There is never more than one liquidus minimum in the

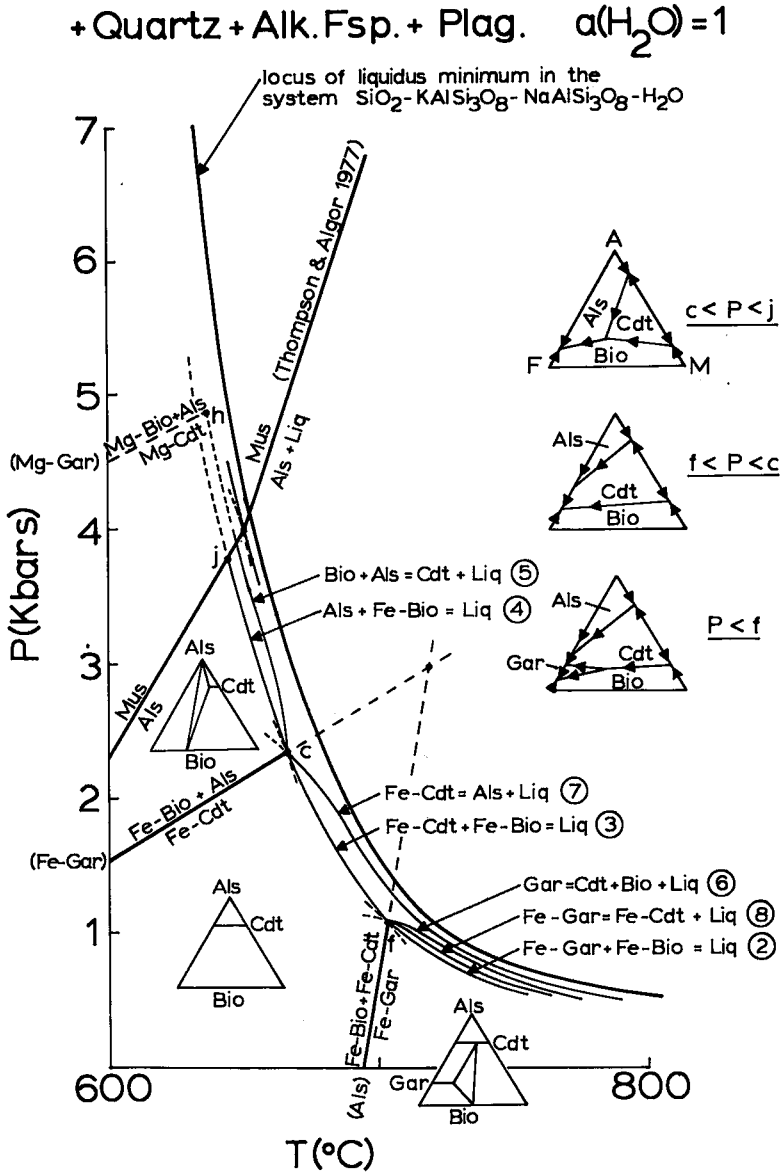

FIG. 2. Stable equilibria for $a(H_2O) = 1.0$ at higher temperatures than the breakdown of muscovite (Thompson & Algor 1977). The intersections of the stable subsolidus reactions and the locus of liquidus minima (points f and c) divide the locus of minima into three segments ($P < f$, $f < P < c$, $c < P < j$). In each pressure regime, the liquidus surface is different in the AFM projection. The locus of liquidus minima in the simple system $KAlSi_3O_8$–$NaAlSi_3O_8$–SiO_2–H_2O is from Tuttle & Bowen (1958).

AFM projection for a given P and $a(H_2O)$. (2) The ratio FeO/MgO is always higher in the liquid than in the coexisting mineral or mineral assemblage. The liquidus minimum lies on the AF join of the AFM projection. It is well known that Fe-end-member minerals are less refractory than their Mg analogues. Also, the liquidus minimum has a high F/A ratio. Aluminosilicate (Al_2SiO_5) is considerably more refractory than FeO-bearing minerals in simple systems (*e.g.*, (FeO–SiO_2–Al_2O_3: Osborn & Muan 1960). This favors a high FeO/Al_2O_3 ratio for the liquidus minimum in any system containing these components. (3) Biotite and Al_2SiO_5 apparently melt congruently in the AFM projection. This is reasonable insofar as these minerals bound the accessible regions of the AFM projection. (4) At low pressures, Mg–cordierite melts congruently in the presence of quartz and feldspar. This has been shown by Schairer (1954) and Schairer & Yoder (1958). (5) Where a liquidus field for Fe–garnet (almandine) first appears in the AFM projection, Fe–garnet melts incongruently. In regions of P–T–$a(H_2O)$ space where Fe–garnet is not stable in any of the possible subsolidus assemblages (Fig. 1), there can be no liquidus field for Fe–garnet in the AFM projection. But, where Fe-garnet does appear in one of the possible subsolidus assemblages, a liquidus field for Fe–garnet is possible. It follows that there are two regions of P–T–$a(H_2O)$ space; in one region, a liquidus field for Fe–garnet is possible; in the other, a liquidus field for Fe–garnet is never possible. The two regions are separated by a surface in P–T–$a(H_2O)$ space marking the first appearance of Fe–garnet in the subsolidus AFM topologies. Where this surface meets the solidus, Fe–garnet must melt incongruently. If this were not so, the projected AFM composition of the liquidus minimum and Fe–garnet would have to be the same everywhere the subsolidus surface met the solidus, a highly improbable situation and therefore an unreasonable constraint to place on the model (see Ehlers 1972, p. 126).

The same argument can be made for Fe–cordierite, so that when a liquidus field for Fe–cordierite first appears in the AFM projection, Fe–cordierite melts incongruently.

It follows from assumptions (1) and (2) that Fe–cordierite coexisting with quartz and feldspar melts incongruently to Al_2SiO_5 plus liquid. And it follows that Fe–garnet (almandine) coexisting with quartz and feldspar must melt incongruently to Al_2SiO_5 + silicate liquid or cordierite + silicate liquid.

At low pressures (P < f in Fig. 2), the minimum-melting reaction is (in terms of AFM minerals only):

$$P < f \qquad \text{Fe–Gar} + \text{Fe–Bio} = \text{Liq} \qquad (2)$$

Where P > f, garnet is unstable relative to annite + Al_2SiO_5 or annite + cordierite. In this pressure range the minimum-melting reactions are:

$$f < P < c \qquad \text{Fe–Cdt} + \text{Fe–Bio} = \text{Liq} \qquad (3)$$

$$P > c \qquad \text{Als} + \text{Fe–Bio} = \text{Liq} \qquad (4)$$

At a higher temperature than the minimum a ternary peritectic reaction is encountered, except where f < P < c:

$$P > c \qquad \text{Bio} + \text{Als} = \text{Cdt} + \text{Liq} \qquad (5)$$

$$< P < c \qquad \text{no ternary peritectic}$$

$$P < f \qquad \text{Gar} = \text{Cdt} + \text{Bio} + \text{Liq} \qquad (6)$$

Where P < c, one or two binary peritectic reactions are encountered on the AF join, depending on the pressure:

$$f < P < c \qquad \text{Fe–Cdt} = \text{Als} + \text{Liq} \qquad (7)$$

$$P < f \qquad \text{Fe–Gar} = \text{Fe–Cdt} + \text{Liq} \qquad (8)$$

$$\text{Fe–Cdt} = \text{Als} + \text{Liq} \qquad (7)$$

The P–T locus of the liquidus-minimum reactions is shown in Figure 2 along with selected higher-temperature liquidus reactions. On the inset AFM liquidus diagrams, the reader should note the gradual shrinkage of the cordierite liquidus field with increasing pressure. The relative positions of the various reactions are correct according to Schreinemakers' rules and the assumptions presented earlier in this section.

Where the activity of H_2O is low, the temperature of the liquid-absent invariant point in the Fe–end-member system is lower than the liquidus minimum. The case for $a(H_2O) \sim P(H_2O)/P(\text{total}) = 0.6$ is shown in Figure 3 along with the subsolidus AFM topologies. Two of the subsolidus reactions meet the liquidus surface at a slightly higher temperature than the liquidus minimum; one of the subsolidus reactions meets the liquidus minimum. Hence, four pressure regimes may be defined, P > d, a < P < d, b < P < a and P < b.

In this case, $a(H_2O) \sim 0.6$, there are two types of minimum reactions:

$$P < d \qquad \text{Fe–Bio} + \text{Fe–Gar} = \text{Liq} \qquad (2)$$

$$P > d \qquad \text{Fe–Bio} + \text{Als} = \text{Liq} \qquad (4)$$

Just above the temperature of the liquidus minimum, one or two ternary peritectic reactions are encountered, depending on the pressure:

$P > d$ Bio + Als = Cdt + Liq (5)

$a < P < d$ Gar = Bio + Als + Liq (9)
Bio + Als = Cdt + Liq (5)

$b < P < a$ Gar = Bio + Cdt + Liq (6)
Gar + Als = Cdt + Liq (10)

$P < b$ Gar = Bio + Cdt + Liq (6)

Where $P < d$, one or two binary peritectic reactions are encountered on the AF join, depending on the pressure:

$b < P < d$ Fe–Gar = Als + Liq (11)

$P < b$ Fe–Gar = Fe–Cdt + Liq (8)
Fe–Cdt = Als + Liq (7)

As $a(H_2O)$ is varied, the point a traces out the locus of the five-phase equilibrium AFM assemblage:

Bio – Gar – Cdt – Als – Liq (12)

Lee & Holdaway (1978) indicated that the locus of this assemblage terminates at an $a(H_2O) \sim P(H_2O)/P(total)$ slightly higher than 0.8, at P(total) = 2750 bars and T = 675°C. At lower pressures the five-phase equilibrium is not encountered.

The other points so far located (b, d, f and c) trace out loci with varying $a(H_2O)$. The various loci terminate at e, the low-pressure end-point of the five-phase equilibrium (12).

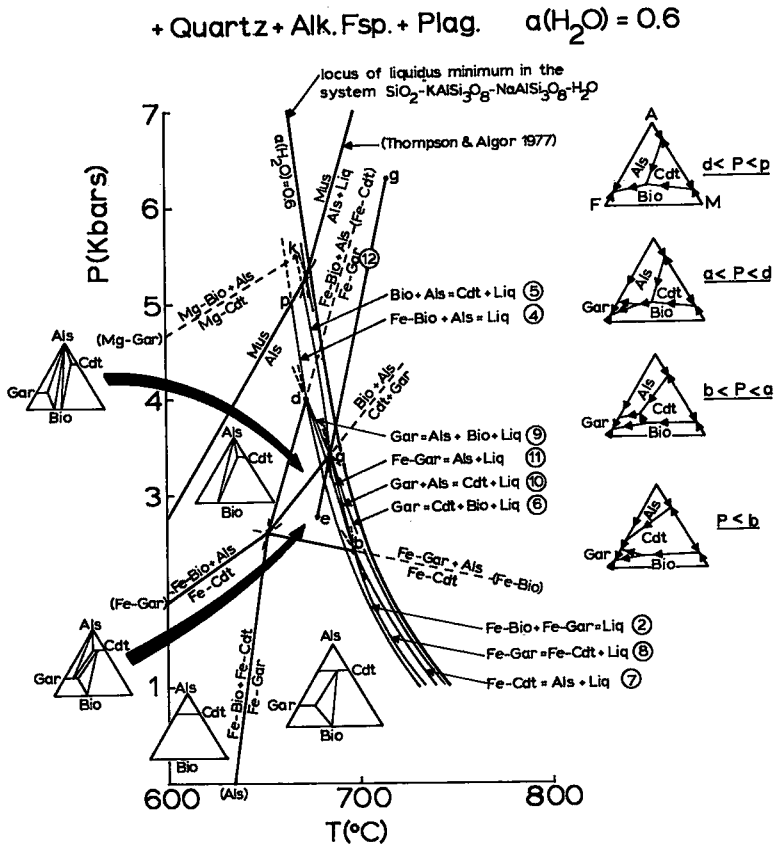

FIG. 3. Stable equilibria for $a(H_2O) = 0.6$ in the AFM projection at higher temperatures than muscovite stability. The locus of liquidus minima in the simple system $KAlSi_3O_8$–$NaAlSi_3O_8$–SiO_2–H_2O, $a(H_2O) = 0.6$ is from Kerrick (1972). The liquidus surface is intersected by three subsolidus reactions, creating four pressure regimes ($P < b$, $b < P < a$, $a < P < d$, $d < P < m$), each having a distinct AFM liquidus topology.

The equilibrium assemblages (coexisting with quartz, plagioclase and alkali feldspar) along each of the five loci are as follows:

(*ea*)	Bio – Gar – Cdt – Als – Liq	(12)
(*eb*)	Fe–Gar – Als – Fe–Cdt – Liq	(13)
(*ef*)	Fe–Bio – Fe–Cdt – Fe–Gar – Liq	(14)
(*ec*)	Fe–Cdt – Fe – Bio – Als – Liq	(15)
(*ed*)	Fe–Gar – Fe–Bio – Als – Liq	(16)

These equilibrium assemblages separate P–T regions of distinct liquidus topology where a (H_2O) < 1. The various liquidus topologies are shown in Figure 4.

There is no liquidus field for cordierite at higher pressures than the line *ng*, the Mg analogue of the Fe-end-member equilibrium *ec* (15). The lines *ec* and *ng* mark the disappearance of a liquidus field for cordierite in the Fe- and Mg-end-member systems, respectively. The line *ng* was located using the data of Lee & Holdaway (1978) in the same way as for *ec*.

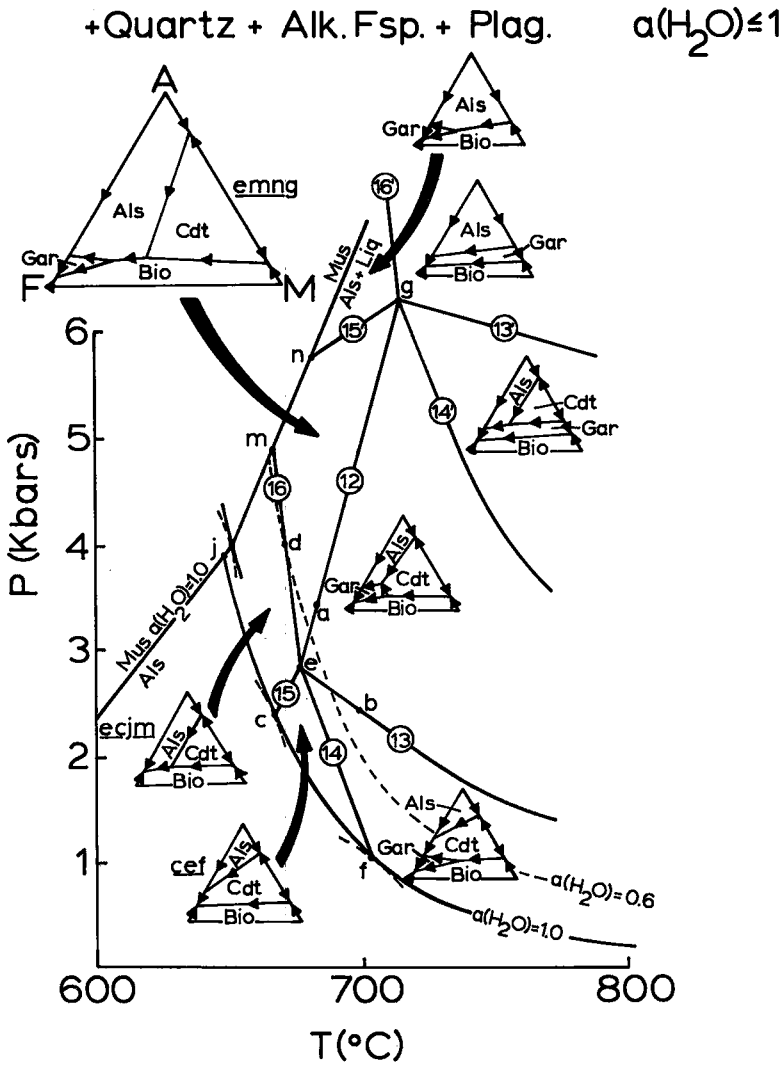

FIG. 4. Regions of distinct AFM liquidus topology in P–T space as a function of $a(H_2O)$. Lines 13′, 14′, 15′ and 16′ represent four-phase liquidus equilibria in the Mg-end-member system, analogous to equilibria 13, 14, 15 and 16, respectively, in the Fe-end-member system.

It is unlikely that the liquidus field for cordierite disappears at the same composition as cordierite. Therefore, shortly before the cordierite field disappears there must be an interval of pressure over which Mg–cordierite melts incongruently to Al_2SiO_5 plus silicate liquid. Presumably, there is a univariant equilibrium (not shown in Fig. 4) dividing P–T space into two regions; in the low-pressure region Mg–cordierite melts congruently (Schairer 1954, Schairer & Yoder 1958); in the high-pressure region, close to the pressure above which there is no liquidus field for cordierite, Mg–cordierite melts incongruently.

Discussion

As long as the silicate liquid is in equilibrium with two feldspars and quartz, the liquidus surface in the AFM projection will correspond approximately to one of the topologies in Figure 4. It should be emphasized that for a given P and $a(H_2O)$ the temperature difference between the liquidus minimum in the system SiO_2–$KAlSi_3O_8$–$NaAlSi_3O_8$ and the liquidus minimum in the AFM projection is less than something of the order of 20°C (Appendix). However, where the silicate liquid is undersaturated with respect to H_2O, [$a(H_2O) < 1$], melting or crystallization proceeds with a complementary decrease or increase in $a(H_2O)$, respectively; the liquid may remain in equilibrium with two feldspars and quartz over a much wider range of temperature. In many cases the liquid may coexist with quartz and two feldspars (an alkali feldspar and an oligoclase or andesine) throughout the crystallization history. Many migmatite terranes from which granitic liquids are believed to have been extracted contain quartz, two feldspars and one or more of the AFM minerals: biotite, cordierite, garnet or Al_2SiO_5. There seems to be a general indication that silicate liquids produced during high-grade metamorphism rarely, if ever, become strongly undersaturated with respect to all of the AFM minerals present in the source rocks.

In high-grade metamorphic rocks, most if not all H_2O is present in the form of hydrated phases such as muscovite, biotite or hornblende. Whatever free H_2O is available in the form of a vapor phase most likely could not saturate a significant volume of silicate liquid. More likely, the bulk of the silicate liquid is produced when muscovite or some other hydrated phase breaks down at a temperature above the locus of H_2O-saturated minima (Fyfe 1969).

A liquid formed as the result of the breakdown of muscovite, for instance, can have an $a(H_2O)$ substantially less than one (Thompson & Algor 1977). The initial liquid will be saturated with respect to all of those minerals present in the rock undergoing melting. Even where present in small modal amounts, it is unlikely that all of the AFM minerals will be melted completely because it takes only a small amount of AFM constituents (of the order of 1 wt. % for MgO or Al_2O_3, somewhat more for FeO) to saturate a liquid already saturated with respect to quartz and one or two feldspars (Bailey 1976, p. 438-439, Bowen 1937, Luth 1967, Roedder 1951, Schairer 1954, Schairer & Bowen 1955, 1956, Schairer & Yoder 1961).

During the melting of a three-phase AFM assemblage, one or two AFM minerals may be melted completely, but it is unlikely that all of the AFM minerals will melt unless the original modal content of the AFM minerals was very low. Where biotite is the most abundant AFM mineral, melting may start at the Gar–Als–Bio peritectic, for instance, but with advanced partial melting the silicate liquid may be wholly within the liquidus field for biotite. After emplacement, the silicate liquid may crystallize to a new assemblage depending on the AFM liquidus topology for the new pressure.

Green (1977) has demonstrated that small amounts of MnO cause a rather dramatic expansion in the stability field for garnet. Unfortunately, the full extent of this effect is not known, as bulk chemical ratios of MgO/(FeO+MgO) less than 0.30 were not considered.

At high temperatures and very low pressures in Figure 4, or where $a(H_2O)$ is very low, fayalite, orthopyroxene or an orthoamphibole (anthophyllite–gedrite) are possible minerals in the subsolidus AFM relationships. Liquidus fields then become possible for one or more of these minerals (Grant 1968, 1973). The new liquidus fields probably appear as a result of the incongruent melting of biotite. This means that the new liquidus fields must extend to at least slightly more aluminous compositions than biotite.

Under most conditions, staurolite is not stable at higher temperatures than the breakdown of muscovite. This was noted by Grant (1973). Hence, a liquidus field for staurolite probably will not appear in the AFM projections in Figure 4. It is interesting to note, however, that staurolite has been reported from at least one location in the Musquodoboit granite pluton

in south-central Nova Scotia (McKenzie & MacGillivary 1974).

Practical Example: South Mountain Batholith, Nova Scotia

The South Mountain batholith (SMB) occupies an area of approximately 10,000 km^2 in southern Nova Scotia. Numerous outlier plutons are found to the east of the main body. The batholith intrudes principally Cambrian-Ordovician shales and greywackes of the Meguma Group. The intrusive contacts are generally discordant and sharp. The Meguma sedimentary rocks have undergone contact metamorphism, and cordierite, garnet and andalusite are common in the metamorphic aureole.

The SMB is composed of at least three intrusive phases (from oldest to youngest): biotite granodiorite, muscovite–biotite adamellite and late-stage pegmatite–aplite associations (McKenzie & Clarke 1975). All the rocks contain quartz, plagioclase, alkali feldspar and biotite in varying proportions. Many areas of the granodiorite and adamellite are characterized by large (up to 10 cm) euhedral, tabular crystals of perthite. The perthite megacrysts contain inclusions of quartz, plagioclase and biotite, even in the very centres of the megacrysts. Plagioclase in the matrix (An_{30-35} in granodiorite, An_{10-30} in adamellite) contains inclusions of quartz, alkali feldspar and biotite. It seems that the silicate liquid associated with these rocks was saturated with respect to two feldspars, quartz and biotite throughout most, if not all, of the crystallization history.

Biotite occurs alone or with one or two of the other AFM minerals. Muscovite occurs as a late-stage (in most cases, subsolidus) replacement after cordierite or andalusite, except in some of the adamellites, where muscovite may be primary. Known assemblages coexisting with quartz and two feldspars (with or without secondary muscovite) are: in the granodiorite, (1) biotite and (2) biotite–cordierite; in the adamellite, (1) biotite–cordierite, (2) biotite–cordierite–andalusite, (3) biotite–andalusite, (4) biotite–garnet and (5) biotite–primary muscovite.

The granodiorite contains well over 5 modal

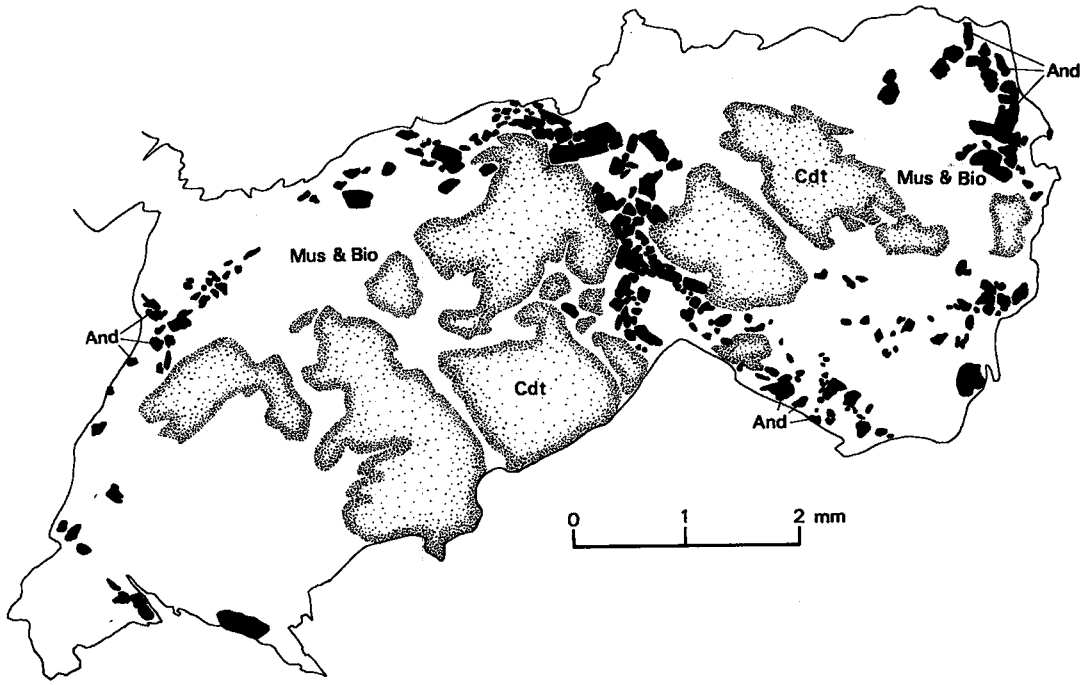

FIG. 5. Cordierite showing andalusite corona, from the Musquodoboit pluton. The cordierite (stippled) has been intensely altered to pinnite. Muscovite and biotite (unornamented) surround the cordierite. Andalusite occurs as minute grains (black) in the muscovite, forming nearly complete coronas around the two principal areas of cordierite.

% mafic constituents. Because a silicate liquid coexisting with quartz and one or two feldspars is unlikely to contain much more than 1% mafic constituents in solution, as discussed in the previous section, the granodiorites may not have been completely liquid, at least at the present level of intrusion. On the other hand, the modal content of AFM minerals in the younger adamellites is very much lower, reinforcing the proposal of McKenzie & Clarke (1975) that these rocks represent a silicate liquid derived from the granodiorite magma.

The andalusites in the biotite–andalusite adamellites occur as small, clear, subhedral crystals, invariably rimmed by secondary muscovite. Clarke *et al.* (1976) have presented evidence to show that the andalusites crystallized directly from the silicate liquid.

Cordierite occurs in both the adamellites (in the Musquodoboit pluton, an outlier to the east of the SMB), and in the granodiorite of the main body. The cordierites form stubby, euhedral to subhedral phenocryysts up to 6 or 7 mm in diameter, very different from the 2-to-3-mm anhedral cordierites found in contact metamorphosed Meguma rocks.

Cordierites in the Musquodoboit pluton are almost invariably rimmed and partly replaced by secondary muscovite. The muscovite is in cases poikilitic, with inclusions of primary andalusite (Fig. 5). Evidently, prior to the growth of the muscovite, the cordierites were surrounded by minute grains of andalusite, giving rise to "corona structures". Biotite occurs as inclusions in the cordierite and with the andalusite forming the coronas. This texture is consistent with the peritectic reaction 5: Bio + Als = Cdt + Liq.

A garnet-bearing muscovite–biotite granite has been reported from the Shelburne pluton (Albuquerque 1977), located just south of the western end of the SMB. The garnet-bearing granite appears to be one of the latest and most differentiated of the rocks examined by Albuquerque (1977). There are a number of late, garnet-rich aplites in the same area. Garnet-bearing pegmatite segregations have been reported from the eastern part of the SMB near the town of Aspotogan.

The various two- and three-phase AFM assemblages are consistent with the liquidus topologies for the P–T region *emng* of Figure 4. The liquid-line-of-descent is conceived of as follows. Throughout most of the batholith, the silicate liquid associated with the granodiorite was in the primary liquidus field for biotite. Through continued crystallization of biotite, the liquid reached the biotite–cordierite liquidus boundary. Once on the boundary, biotite and cordierite crystallized together.

When the adamellite liquid evolved from the granodiorite magma, the silicate liquid was saturated with respect to biotite, or biotite and cordierite, depending on the local AFM composition of the liquid. Some adamellites (Musquodoboit pluton) crystallized for a time on the biotite–cordierite liquidus boundary. Invariably the cordierites are rimmed by muscovite and pinnite or muscovite with poikilitically enclosed andalusite. Although most of the pinnite and muscovite seems to be due to late-stage, subsolidus replacement of the cordierites or rimming andalusite, at least some of the muscovite may have crystallized at the four-phase peritectic reaction:

$$\text{Bio} + \text{Mus} = \text{Cdt} + \text{Liq} \qquad (17)$$

(Compare with reaction 5.)

Most of the adamellites contain biotite–andalusite, biotite–muscovite, biotite–cordierite or biotite–cordierite–andalusite, the last assemblage being peritectic. The three-phase assemblage biotite–garnet–andalusite has not been encountered in the adamellites. However, the late and highly differentiated biotite–garnet granites described by Albuquerque (1977) suggest that the three-phase assemblage biotite–garnet–andalusite is most likely peritectic.

The sequence of AFM assemblages in the granodiorites and adamellites indicates that the region *emng* of Figure 4 defines the appropriate set of conditions for the crystallization of the SMB. The approximate temperature range was 675 to 725°C; the approximate pressure range was 3 to 6 kbar. This is consistent with previously estimated conditions based on the occurrence of primary andalusite in parts of the SMB (Clarke *et al.* 1976). Our analysis suggests that the $a(H_2O)$ was less than one in the silicate liquids associated with the SMB. Either the silicate liquids were undersaturated with respect to a vapor phase or more likely, if saturated, the vapor phase was not pure H_2O.

Acknowledgements

The principal author (RNA) is grateful for the generous support of the Sir Isaac Walton Killam Foundation of Dalhousie University.

References

ABBOTT, R. N., JR. (1978): Peritectic reactions in the system An–Ab–Or–Qz–H_2O. *Can. Mineral.* **16**, 245-256.

ALBUQUERQUE, C. A. R. DE (1977): Geochemistry of the tonalitic and granitic rocks of the Nova Scotia southern plutons. *Geochim. Cosmochim. Acta* **41**, 1-13.

BAILEY, D. K. (1976): Applications of experiments to alkaline rocks. *In* The Evolution of the Crystalline Rocks (D. K. Bailey & R. MacDonald, eds.), Academic Press, London.

BOWEN, N. L. (1937): Recent high-temperature research on silicates and its significance in igneous geology. *Amer. J. Sci.* **233**, 1-21.

CLARKE, D. B., MCKENZIE, C. B., MUECKE, G. K. & RICHARDSON, S. W. (1976): Magmatic andalusite from the South Mountain batholith, Nova Scotia. *Contr. Mineral. Petrology* **56**, 279-287.

EHLERS, E. G. (1972): *The Interpretation of Geological Phase Diagrams.* W. H. Freeman & Co., San Francisco.

FYFE, W. S. (1969): Some thoughts on granitic magmas. *In* Mechanism of Igneous Intrusion (G. Newall & N. Rast, eds.), *Geol. J. Spec. Issue* **2**.

GRANT, J. A. (1968): Partial melting of common rocks as a possible source of cordierite-anthophyllite bearing assemblages. *Amer. J. Sci.* **266**, 908-931.

——— (1973): Phase equilibria in high-grade metamorphism and partial melting of pelitic rocks. *Amer. J. Sci.* **273**, 289-317.

GREEN, T. H. (1977): Garnet in silicic liquids and its possible use as a P–T indicator. *Contr. Mineral. Petrology* **65**, 59-67.

JAMES, R. S. & HAMILTON, D. L. (1969): Phase relations in the system $NaAlSi_3O_8$–$KAlSi_3O_8$–$CaAl_2Si_2O_8$–SiO_2 at 1 kilobar water vapor pressure. *Contr. Mineral. Petrology* **21**, 111-141.

KERRICK, D. M. (1972): Experimental determination of muscovite + quartz stability with $PH_2O < P_{total}$. *Amer. J. Sci.* **272**, 946-958.

LEE, SANG MAN & HOLDAWAY, M. J. (1978): Significance of Fe–Mg cordierite stability relations on temperature, pressure, and water pressure in cordierite granulites. *In* The Earth's Crust: its Nature and Physical Properties (J.G. Heacock, ed.). *Amer. Geophys. Union Mon.* **20**, 79-94.

LUTH, W. C. (1967): Studies in the system $KAlSiO_4$–Mg_2SiO_4–SiO_2–H_2O. I. Inferred phase relations and petrologic applications. *J. Petrology* **8**, 372-416.

MCKENZIE, C. B. & CLARKE, D. B. (1975): Petrology of the South Mountain batholith, Nova Scotia, *Can. J. Earth Sci.* **12**, 1209-1218.

——— & MACGILLIVARY, J. (1974): *Eastern Nova Scotia Granites Project,* Dep. Geology, Dalhousie Univ., Halifax, N.S.

OSBORN, E. F. & MUAN, A. (1960): *Phase Equilibrium Diagrams of Oxide Systems. The System "FeO"–Al_2O_3–SiO_2.* Amer. Ceramic Soc. and Edward Orton Jr. Ceramic Found., Columbus. Ohio, Plate **9**.

RICCI, J. E. (1951): *The Phase Rule and Heterogeneous Equilibrium.* Van Nostrand, New York.

ROEDDER, E. (1951): Low temperature liquid immiscibility in the system K_2O–FeO–Al_2O_3–SiO_2. *Amer. Mineral.* **36**, 282-286.

SCHAIRER, J. F. (1950): The alkali-feldspar join in the system $NaAlSiO_4$–$KAlSiO_4$–SiO_2. *J. Geol.* **58**, 512-517.

——— (1954): The system K_2O–MgO–Al_2O_3–SiO_2. I. Results of quenching experiments on four joins in the tetrahedron cordierite–forsterite–leucite–silica and on the join cordierite–mullite–potash feldspar. *J. Amer. Ceramic Soc.* **37**, 501-533.

——— (1957): Melting relations of the common rock-forming oxides. *J. Amer. Ceramic Soc.* **40**, 215-239.

——— & BOWEN, N. L. (1955): The system K_2O–Al_2O_3–SiO_2. *Amer. J. Sci.* **253**, 681-746.

——— & ——— (1956): The system Na_2O–Al_2O_3–SiO_2. *Amer. J. Sci.* **254**, 129-195.

——— & YODER, H. S., JR. (1958): The quaternary system Na_2O–MgO–Al_2O_3–SiO_2. *Carnegie Inst. Wash. Yearb.* **57**, 210-212.

——— & ——— (1961): Crystallization in the system nepheline–forsterite–silica at one atmosphere pressure. *Carnegie Inst. Wash. Yearb.* **60**, 141-144.

THOMPSON, A. B. & ALGOR, J. R. (1977): Model systems for anatexis of pelitic rocks. I. Theory of melting reactions in the system $KAlO_2$–$NaAlO_2$–Al_2O_3–SiO_2–H_2O. *Contr. Mineral. Petrology* **63**, 247-269.

THOMPSON, J. B., JR. (1957): The graphical analysis of mineral assemblages in pelitic schists. *Amer. Mineral.* **42**, 842-858.

TUTTLE, O. F. & BOWEN, N. L. (1958): The origin of granite in the light of experimental studies in the system $NaAlSi_3O_8$–$KAlSi_3O_8$–SiO_2–H_2O. *Geol. Soc. Amer. Mem.* **74**.

Received October 1978; revised manuscript accepted December 1978.